Journal of Magnetism and Magnetic Materials 497 (2020) 165984

Contents lists available at ScienceDirect

Journal of Magnetism and Magnetic Materials

journal homepage: www.elsevier.com/locate/jmmm

Research articles

Magnetism and electrical conductivity of molecular semiconductor, $[Fe^{II}(DMF)_4(TCNQ)_2](TCNQ)_2$, with fractionally charged TCNQ units

Ökten Üngör[a,1], Hoa Phan[a,b,1], Eun Sang Choi[c], Judith K. Roth[a], Michael Shatruk[a,*]

[a] Department of Chemistry and Biochemistry, Florida State University, 95 Chieftan Way, Tallahassee, FL 32306, USA
[b] Department of Chemistry, Vinh University, 182 LeDuan Street, Vinh City, Viet Nam
[c] National High Magnetic Field Laboratory, 1800 E Paul Dirac Dr, Tallahassee, FL 32310, USA

ARTICLE INFO

Keywords:
Molecular conductors
TCNQ
Pi-pi stacking
One-dimensional structures
Coordination chemistry

ABSTRACT

We report the synthesis of a semiconducting material, $[Fe^{II}(DMF)_4(TCNQ)_2](TCNQ)_2$ (**1**), which contains partially charged $TCNQ^{\delta-}$ anions (TCNQ = 7,7,8,8-tetracyanoquinodimethane, $0 < \delta < 1$). Compound **1** was prepared by different routes, using $(Et_3NH)(TCNQ)_2$, a mixture of TCNQ and LiTCNQ, or a mixture of TCNQ and NaTCNQ, to obtain the structure with fractionally charged $TCNQ^{\delta-}$ anions. The crystal structure of **1** is formed by mononuclear cations $[Fe(DMF)_4(TCNQ)_2]^{2\delta+}$, the TCNQ units of which form infinite π-π stacks with non-coordinated $TCNQ^{\delta-}$ counter ions. A detailed examination of X-ray diffraction data, supplemented by inductively coupled plasma mass spectrometry, indicates that some of the non-coordinated $TCNQ^{\delta-}$ anions, likely, form bonds to a partially occupied Na^+ site, thus causing slightly different crystal packing in the vicinity of some Fe(II) centers. This finding is indirectly corroborated by the results of Mössbauer spectroscopy, which shows that the transition metal site corresponds to the high-spin Fe(II) ion, but two such sites are present, with slightly different quadrupole splitting parameters. Temperature-dependent conductivity measurements reveal semiconducting behavior, with the room-temperature conductivity of 0.125 S/cm and the charge-hopping activation energy of 180 meV.

1. Introduction

The charge-transfer salt between the organic donor, tetrathiafulvalene (TTF), and organic acceptor, 7,7,8,8-tetracyanoquinodimethane (TCNQ), arguably, is the most well-known organic metal [1]. Its excellent conducting properties are explained by the partial donor-acceptor charge transfer, which is typically expressed as $(TTF)^{\delta+}(TCNQ)^{\delta-}$, where $\delta \approx 0.55$ [2]. The formation of stacks of fractionally charged anions lowers the on-site Coulomb repulsion (U) and increases the transfer integral (t), which facilitates charge hopping along the stacks, leading to the high conductivity values. Following the discovery of the metallic behavior in TTF-TCNQ, this principle has been realized in many other donor-acceptor combinations [3,4], as well as in charge-transfer salts, where the conducting organic part of the structure is co-crystallized with inert ("spectator") counter ions [5,6]. Such studies led to the discovery of superconductivity in the charge-transfer salts of tetramethyltetraselenafulvalenium (TMTSF) [7,8] and later in other related materials [9]. The counter ions can be also used to impart another function to the material, thus leading to multifunctionality [10,11]. For example, fractionally charged cations based on TTF and related organic donors have been co-crystallized with various metal-containing anions to obtain paramagnetic molecule-based conductors [12,13]. At the same time, there are significantly fewer examples of structurally characterized materials composed of paramagnetic metal-containing cationic complexes and fractionally charged anions based on TCNQ or its analogues [14–21].

In addition to their ability to form efficient charge-transporting pathways, organonitrile molecules such as TCNQ also readily act as bridging ligands, which is known to cause significant difficulties in crystallizing their salts with transition metal ions [22–26]. This problem can be circumvented by the use of blocking ligands or co-ordinating solvents, which completely or partially prevent coordination of TCNQ to the metal center. For example, *N*,*N*-dimethylformamide (DMF) was used effectively to crystallize several coordination polymers formed by metal cations and integer-charged $TCNQ^-$ or $TCNQ^{2-}$ anions, in which DMF acts as either non-coordinating [27–29] or co-ordinating [30] solvent. On the other hand, we and other groups also used DMF as solvent to co-crystallize Fe^{II} or Co^{II} ions, completely

* Corresponding author.
E-mail address: shatruk@chem.fsu.edu (M. Shatruk).
[1] Both authors contributed equally to this work.

https://doi.org/10.1016/j.jmmm.2019.165984
Received 15 March 2019; Received in revised form 17 July 2019; Accepted 12 October 2019
Available online 14 October 2019
0304-8853/

protected by blocking ligands, with fractionally charged $TCNQ^{\delta-}$ anions in order to obtain highly conducting materials that exhibits spin crossover at the transition metal center [31–33]. Incited by these examples, we decided to explore the formation of complexes between the Fe^{2+} cations and fractionally charged $TCNQ^{\delta-}$ anions in the DMF solution in the absence of any other co-ligands. Reported herein are the synthesis, crystal structure, and physical properties of a paramagnetic semiconductor, $[Fe(DMF)_4(TCNQ)_2](TCNQ)_2$, which exhibits high electrical conductivity.

2. Materials and methods

2.1. Synthesis

All reactions were performed under an inert N_2 atmosphere using standard Schlenk techniques. All reagents and anhydrous solvents were purchased from Aldrich, except for TCNQ, which was obtained from TCI America. The $(Et_3NH)(TCNQ)_2$, LiTCNQ, and NaTCNQ precursors were prepared according to the published procedures [34,35]. Elemental analysis was performed by Atlantic Microlab, Inc. (Norcross, GA, USA). Thermal gravimetric analysis (TGA) was performed on the TA Instruments Q50 Thermogravimetric Analyzer, in the temperature range from 25 to 900 °C, at a heating rate of 5 °C/min.

2.2. $[Fe(DMF)_4(TCNQ)_2](TCNQ)_2$ (1)

Method A – using $(Et_3NH)(TCNQ)_2$. A solution of 12.8 mg (0.0379 mmol) of $[Fe(BF_4)_2]\cdot 6H_2O$ in 1.0 mL of anhydrous DMF was added via a cannula to a solution of 38.3 mg (0.0751 mmol) of $(Et_3NH)(TCNQ)_2$ in 3.0 mL of anhydrous acetone. The mixture was stirred for 10 min at room temperature (R.T.), resulting in a dark-green solution, which was layered with diethyl ether (Et_2O) to afford needle-shaped dark-green crystals of **1** after one day. The product was collected by filtration, washed with Et_2O, and dried by suction. Yield = 16.5 mg (37.4%). *IR*(cm^{-1}), ν(C≡N): 2218, 2214, 2154; ν(C=N): 1506; ν(C−H): 835. *Elem. analysis*: calcd. (found) for **1**·0.5DMF ($FeO_{4.5}N_{20.5}C_{61.5}H_{47.5}$): C 61.48 (61.19), H 3.98 (3.98), N 23.90 (23.92).

Two alternative methods were used to obtain crystals of **1**:

Method B – using LiTCNQ. A solution of 16.9 mg (0.0500 mmol) of $[Fe(BF_4)_2]\cdot 6H_2O$ in 1.0 mL of anhydrous DMF was added via a cannula to a solution of 21.2 mg (0.100 mmol) of LiTCNQ and 20.4 mg (0.0990 mmol) of TCNQ in 3.0 mL of anhydrous acetone. The mixture was stirred for 30 min at R.T., resulting in a dark-green solution, which was layered with Et_2O to afford needle-shaped dark-green crystals of **1** after one day. The product was collected by filtration, washed with Et_2O, and dried by suction. Yield = 18.7 mg (32.1%).

Method C – using NaTCNQ. This method was analogous to Method B, using $[Fe(BF_4)_2]\cdot 6H_2O$ (16.9 mg, 0.0500 mmol) in 1.0 mL of DMF and NaTCNQ (22.7 mg, 0.0990 mmol) and TCNQ (20.4 mg, 0.0999 mmol) in 3.0 mL of acetone. The product was collected by filtration, washed with Et_2O, and dried by suction. Yield = 18.0 mg (31.0%).

2.3. X-Ray Crystallography.

Single-crystal X-ray diffraction was performed on a Bruker APEX-II diffractometer equipped with a CCD detector and a graphite-monochromated Mo-*Kα* radiation source (λ = 0.71073 Å). A single crystal of **1** was suspended in Paratone-N oil (Hampton Research) and mounted on a cryoloop which was cooled to 100 K in an N_2 cold stream. The data set was recorded as *ω*-scans at 0.3° step width and integrated with the Bruker SAINT software package [36]. A multi-scan adsorption correction was applied based on multiple equivalent measurements (SADABS) [37]. The space group was determined with XPREP [38], and the crystal structure solution and refinement were carried out using the SHELX software [39]. The final refinement was performed with anisotropic atomic displacement parameters (ADPs) for all non-hydrogen atoms. All H atoms were placed in calculated positions and refined in the riding model. Further discussion of the refinement procedure is provided in Section 3.2. Full details of the crystal structure refinement and the final structural parameters have been deposited with the Cambridge Crystallographic Data Centre (CCDC). The CCDC registry number and a brief summary of data collection and refinement are provided in Table 1.

Table 1
Data collection and crystal structure refinement parameters for **1**.

Formula	$FeO_4N_{20}C_{60}H_{44}Na_{0.18}$ (**1**)
CCDC number	1897663
T, K	100(1)
Molar mass, g/mol	1169.14
Space group	$P\bar{1}$
a, Å	9.1832(7)
b, Å	10.7689(8)
c, Å	14.916(1)
α, deg	96.123(1)
β, deg	93.812(1)
γ, deg	101.202(1)
V, Å^3	1433.0(2)
Z	1
Crystal color/shape	dark-green plate
Crystal size	0.28 × 0.26 × 0.15
d_{calc}, g cm^{-3}	1.355
μ, mm^{-1}	0.332
λ, Å	0.71073
$2\theta_{max}$, deg	28.56
Total reflections (R_{int})	16,602 (0.056)
Unique reflections	6635
Parameters refined	390
Restraints used	0
R_1, wR_2 [$I > 2\sigma(I)$][a]	0.052, 0.136
R_1, wR_2 (all data)	0.080, 0.155
Goodness of fit[b]	1.080
Diff. peak/hole, e Å^{-3}	0.70, –0.48

[a] $R_1 = \Sigma||F_o|-|F_c||/\Sigma|F_o|$; $wR_2 = [\Sigma[w(F_o^2-F_c^2)^2]/\Sigma[w(F_o^2)^2]]^{1/2}$.
[b] Goodness-of-fit = $[\Sigma[w(F_o^2-F_c^2)^2]/(N_{obs}-N_{params})]^{1/2}$, based on all data.

2.4. Mössbauer spectroscopy

^{57}Fe Mössbauer spectra were collected on a constant acceleration instrument at 278 K. A neat polycrystalline sample of **1** was placed directly in a custom-made polyethylene cup and closed with a lid. Isomer shifts are quoted relative to Fe metal foil at R.T. The spectra were simulated with the MossA software [40].

2.5. Inductively coupled plasma mass spectrometry (ICP-MS)

The ICP-MS measurements were performed on a single-quadrupole iCAP RQ spectrometer (Thermo Fischer Scientific). Samples were prepared by dissolving 2.5, 10.0, and 20.0 mg of **1** in 100 mL of 2% HNO_3 to achieve, respectively, 25, 100, and 200 ppm concentrations of the complex. The content of Li^+ and Na^+ ions was subsequently determined against calibration curves obtained with a commercial Li standard (Aldrich) and a Na standard prepared in house.

2.6. Transport measurements

Electrical resistance was measured on single-crystal samples of **1**, with a typical crystal size around 0.4 × 0.3 × 0.08 mm^3. A 4-probe measurement setup was used, with current being applied parallel to the long direction of the plate-like crystal. The direct current (dc) was applied by means of a Keithley 6221 source while a Keithley 2182 nanovoltmeter or a Keithley 6517A electrometer was used to measure the voltage. The polarity of the dc current was alternated to remove the

thermal emf contribution. The temperature dependence of the resistance was measured using a closed-cycle cryostat while sweeping the temperature at a rate between 1 and 2 K/min.

2.7. Magnetic measurements

Magnetic properties were measured on a polycrystalline sample of **1**, using a superconducting quantum interference device (SQUID) magnetometer MPMS-XL (Quantum Design). Magnetic susceptibility was measured in a dc applied magnetic field of 0.1 T in the 1.8–300 K temperature range. The data were corrected for the diamagnetic contribution from the sample holder and for the intrinsic diamagnetism using tabulated constants [41].

3. Results and discussion

3.1. Synthesis

The reaction between the $[Fe(BF_4)_2]\cdot 6H_2O$ precursor and $(Et_3NH)(TCNQ)_2$, in which TCNQ is already fractionally charged, affords the mononuclear complex $[Fe(DMF)_4(TCNQ)_2](TCNQ)_2$ (**1**), which was crystallized by slow diffusion of Et_2O into the DMF solution of the compound. Complex **1** crystallizes as dark-green elongated plates (or flattened needles), which are sufficiently stable to be handled in air, but gradually degrade upon storage in an open container. The TGA measurements (Fig. S1) showed that the complex loses 23.5% of its mass in the temperature range from 100 to 150 °C, which is attributed to the loss of the coordinated DMF molecules (theoretically 25.1% of the molar mass). Two more decomposition steps are observed upon further heating to 400 °C.

The same complex was also obtained by using a TCNQ/LiTCNQ or TCNQ/NaTCNQ mixture as a precursor, in order to achieve the fractionally charged TCNQ units in the final product through the comproportionation reaction. The use of these precursors was aimed at elucidating the possibility of inclusion of the alkali metal ion into the crystal structure of **1**, as will be discussed below.

3.2. Crystal structure

Complex **1** crystallizes in the triclinic space group $P\bar{1}$. The crystal structure features a mononuclear cationic complex $[Fe(DMF)_4(TCNQ)_2]^{2\delta+}$ co-crystallized with two $TCNQ^{\delta-}$ anions per formula unit (f.u.) (Fig. 1), where $0 < \delta < 1$. Each Fe(II) center lies on an inversion center (0, ½, 0) and is octahedrally coordinated by oxygen atoms of four DMF molecules in the equatorial positions and two nitrogen atoms of TCNQ in the axial positions. Two of the $TCNQ^{\delta-}$ anions ($TCNQ^{C}$) per f.u. coordinate directly to Fe(II) ions while the other two $TCNQ^{\delta-}$ anions ($TCNQ^{U}$) remain non-coordinated and serve as counter ions. The equatorial Fe–O bond lengths are 2.099 and 2.103 Å, while the axial Fe–N bonds are 2.144 Å.

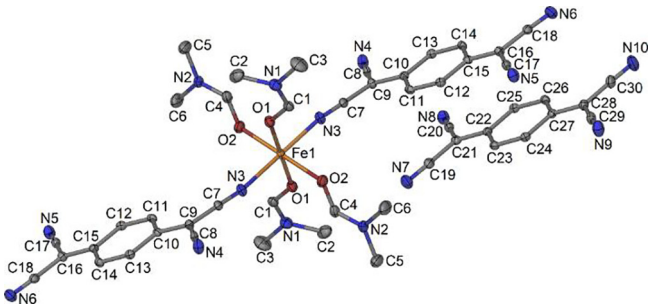

Fig. 1. The crystal structure of **1** (the H atoms are omitted for clarity): the mononuclear $[Fe(DMF)_4(TCNQ)_2]^{2\delta+}$ cation and one of the $TCNQ^{\delta-}$ counter anions, with the atomic displacement ellipsoids at the 50% probability level.

The most notable feature of the crystal structure of **1** are infinite one-dimensional stacks of TCNQ units, which propagate along the [110] crystallographic direction (Fig. 2a). The stacks include the $TCNQ^{C}$ units, terminally coordinated to the Fe^{II} centers of the mononuclear $[Fe(DMF)_4(TCNQ)_2]^{2\delta+}$ cations, and the non-coordinated $TCNQ^{U}$ units (Fig. 2a). The TCNQ units engage in π-π stacking interactions along the column, with the CCUU repeat pattern (Fig. 2). The TCNQ units are parallel to one another in the pairs of coordinated or non-coordinated units, while the planes of the adjacent $TCNQ^{C}$ and $TCNQ^{U}$ are offset by a dihedral angle of 1.1°. The $TCNQ^{C}$–$TCNQ^{U}$ π-π overlaps are of the ring-ring type, with the interplanar distances of 3.113 Å and 3.217 Å between the quinoid planes. The $TCNQ^{C}$–$TCNQ^{C}$ and $TCNQ^{U}$–$TCNQ^{U}$ overlaps are of the ring-external bond type, with the interplanar distances of 3.188 Å and 3.287 Å, respectively. Such parallel arrangement of the TCNQ units, with relatively short distances between them, is a promising pre-requisite for facilitating electron hopping along the stacks, due to the increased transfer integral (t) which should lead to improved electrical conductivity. The other requirement is that the TCNQ units be fractionally charged, in order to decrease the effective-U parameter, $U_{eff} = U - J$, which involves both the on-site electron-electron repulsion U and the exchange interaction J [3,42,43].

The knowledge of the intramolecular distances in the TCNQ units can be used to assign approximate charges to each of these units [31,44], based on the overall electroneutrality of the complex. The presence of the Fe(II) ion has been confirmed by the Mössbauer spectroscopy (described below). However, our crystal structure refinement also suggested the presence of additional electron density located on another inversion center (½,0,0) within the unit cell. Although such peaks, observed on the high-symmetry positions, can occur as artifacts of X-ray diffraction experiments, the peak observed in our experiment was non-negligible, as compared to the other residual peaks observed in the difference Fourier electron density maps. Therefore, we decided to investigate this problem more carefully by preparing complex **1** starting with the precursor mixtures which contained alkali metal ions, i.e., LiTCNQ/TCNQ or NaTCNQ/TCNQ. We performed several single-crystal X-ray diffraction experiments on the crystals isolated from these reactions, as well as on the crystals isolated from the reaction with $(Et_3NH)(TCNQ)_2$ (in the latter method, no alkali-metal-containing reactant were used at any step of the synthesis). Independent of the synthetic method, we consistently observed the significant residual electron density peak in the same position. The height of this peak varied from 1.16 to 4.66 $e^-/Å^3$ and did not show any correlation to the TCNQ precursor used (Table S1).

Several samples of **1**, with the total mass varying from 2.5 to 20 mg, were dissolved in 100 mL of dilute HNO_3 (2% w/w) and analyzed by ICP-MS to establish the possible presence of Li^+ or Na^+ ions. The spectra showed that the concentration of Li^+ ions was negligible (below 20 ppb), irrespective of the amount of **1** that was used (Table S2). On the other hand, the analysis revealed a substantial concentration of Na^+ ions (above 500 ppb). The exact quantification of Na^+ ions in the sample of **1** is challenging due to the presence of these ions even in solutions free of complex **1** (for example, a substantial amount of Na^+ was detected in the commercial Li^+ standard solution). This is a known problem caused by the abundance of adventitious Na^+ ions in solutions stored in glass containers. Importantly, however, we observed a relative increase in the Na^+ concentration when a larger amount of **1** was used for sample preparation (Table S2), which suggests that complex **1** contains Na^+ ions.

The coordination environment of the residual peak in the (½,0,0) site (the green sites in Fig. 3) is a square plane formed by two N atoms of the $TCNQ^{U}$ units, located at the distance of 2.14 Å from the peak, and two methyl H atoms of the DMF molecules, at 1.88 Å. Two more distant methyl H atoms at 2.67 Å might be considered as complementing the coordination to form an elongated octahedron. Such coordination is not unusual for alkali metal ions. Examination of the Cambridge Structural

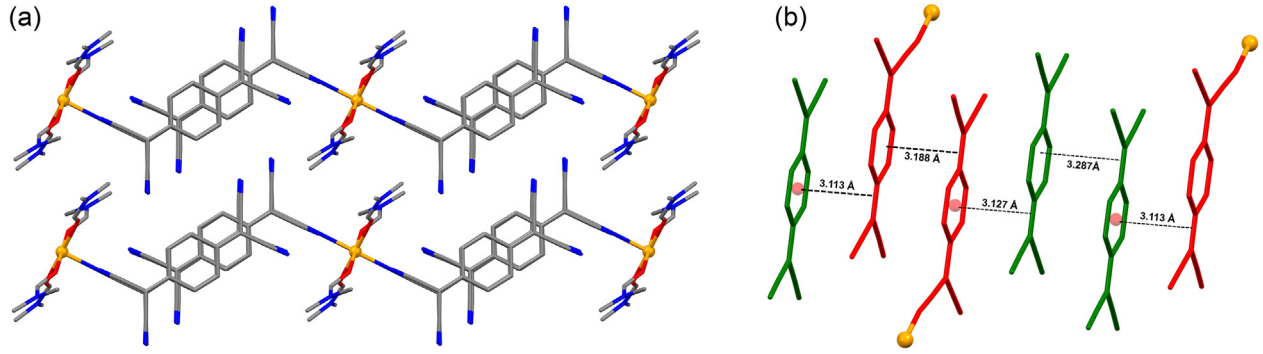

Fig. 2. (a) Top view of the one-dimensional stacks of TCNQ units in the crystal packing of **1**. Color scheme: Fe = orange, O = red, N = blue, C = gray. (b) Side view of a single stack of TCNQ units, with the indication of interplanar distances. Color scheme: Fe = orange, $TCNQ^{C}$ = red, $TCNQ^{U}$ = green. The H atoms are omitted for clarity. (For interpretation of the references to color in this figure legend, the reader is referred to the web version of this article.)

Database shows that the nearest metal-N and metal-H interatomic distances observed for such coordination environment are significantly different in the case of the Li^{+} and Na^{+} ions. The experimental distances are similar to the average Li–N and Li–H distances observed in the reported structures with the Li-[N_2H_2] coordination (Table S3), but attributing the residual electron density to a partially occupied Li site contradicts the results of the IPC-MS measurements, which did not detect any significant amount of Li^{+} ions in the samples of **1**. Therefore, we tentatively assign this residual peak to a partially occupied Na site. The observed peak value was increased for the crystal obtained from the reaction with NaTCNQ / TCNQ, which might serve as an additional evidence for Na^{+} incorporation into the structure. The refinement of the site occupancy factor (SOF) led to variable values, which in general fell below 20%. The SOF value was strongly correlated to the ADP of the Na atom, which was restricted to be isotropic. The SOF value was gradually varied while observing the quality markers of the refinement (the ADP of the Na site, the *R*-factor, the goodness of fit, and the residual electron density). In each structure refined by us, physically meaningful refinement and good quality markers were obtained for a rather narrow range of SOF value, at 10–20%. The low occupancy of this site might also justify the observation of rather short distances for the coordination environment of the Na^{+} ion. In the presence of the Na^{+} ion, the coordinating N and H atoms might be pushed slightly further away from the (½,0,0) site, but in the absence of the Na^{+} ions, these atoms will move closer to the vacancy. Since the (½,0,0) site is dominated by vacancies, the average structure has apparently shorter Na–H and Na–N bond lengths. Unfortunately, we have not been able to detect the existence of any superstructure reflections that would have helped to resolve such a scenario.

Based on all these findings, and on the additional evidence obtained from Mössbauer spectroscopy (see below), we believe that complex **1** should be formulated as $[Fe^{II}(DMF)_4(TCNQ)_2][Na_x(TCNQ)_2]$, with the inclusion of a variable amount of the Na^{+} ions. Therefore, the total charge on the four TCNQ units per f.u. is $-(x + 2)$, and the average charge on each TCNQ unit is slightly more negative than -0.50. The charge on each TCNQ unit can be estimated from the relationship proposed by Kistenmacher *et al.* [44]: $-\delta = -41.67[c/(b + d)] + 19.83$, with the metric parameters defined in Scheme 1. Using the molecular geometries established by crystal structure determination at 100 K, we find that the negative charges on the $TCNQ^{U}$ and $TCNQ^{C}$ units are in the 0.32/0.68 ratio. These charges should be scaled to maintain electroneutrality per f.u. of **1**, and therefore, the calculated charges on $TCNQ^{U}$ and $TCNQ^{C}$ are $-0.16(x + 2)$ and $-0.34(x + 2)$, respectively. As an example, charges of -0.35 and -0.74 are calculated for $x = 0.18$, which was established by the crystal structure refinement for the crystal obtained from the reaction with NaTCNQ/TCNQ. Although the charge distribution is somewhat uneven, the presence of fractional charges and the relatively close interplanar approach of the TCNQ units suggest that complex **1** should exhibit appreciable conductivity in the direction of the TCNQ stacks.

This modified structural model implies that some $TCNQ^{U}$ units become coordinated when the (½,0,0) site is filled with a Na^{+} ion (Fig. 3). Therefore, the crystal packing nearby some of the Fe(II) centers becomes slightly modified due to the presence of the alkali-metal ions.

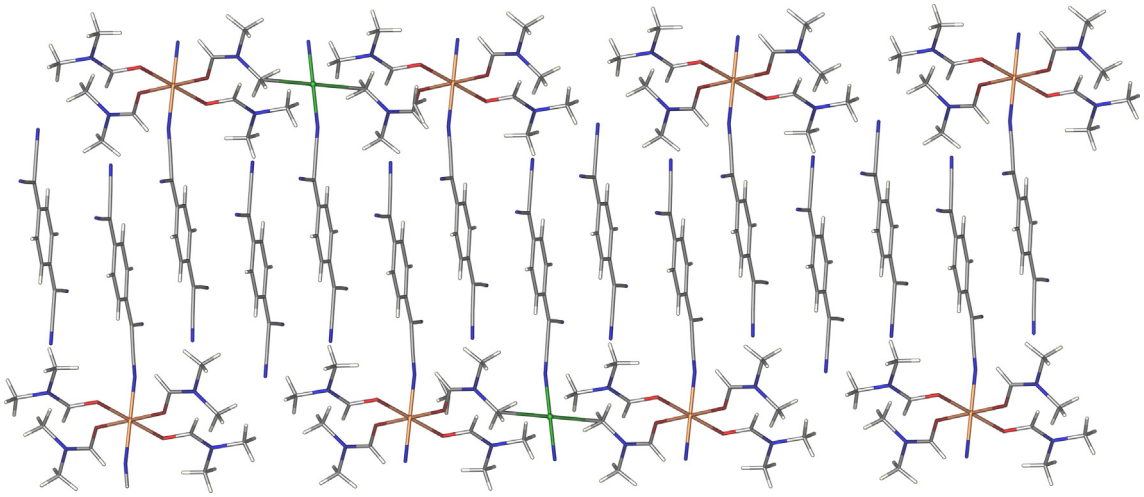

Fig. 3. Crystal packing of **1** modified by the presence of a partially occupied Na site. Color scheme: Fe = orange, Na = green, O = red, N = blue, C = gray, H = beige. (For interpretation of the references to color in this figure legend, the reader is referred to the web version of this article.)

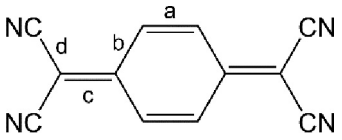

Scheme 1. Metric parameter used in the Kistenmacher equation.

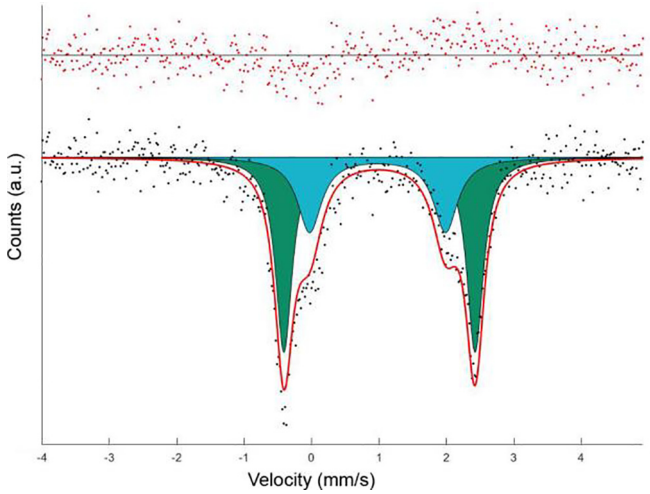

Fig. 4. The Mössbauer spectrum of **1** collected ad 278 K. The shaded areas represent two quadrupole-split spectral components, while the full spectral simulation is shown with a solid red line. The top of the plot shows the residual difference plot obtained after fitting the data. (For interpretation of the references to color in this figure legend, the reader is referred to the web version of this article.)

While X-ray diffraction is insensitive to such minor structural modifications, since it reflects the average crystal structure, Mössbauer spectroscopy can be used as a sensitive probe for subtle local effects of the coordination environment.

3.3. Mössbauer spectroscopy

The Mössbauer spectrum of **1** collected at R.T. (Fig. 4) revealed the presence of a strongly split quadrupole doublet, characteristic of high-spin Fe(II) ions. In addition, components of another, lower-intensity doublet with a similar quadrupole splitting were observed as shoulders present in the larger-intensity doublet. The spectrum was satisfactorily fit with these two doublet components, described with the similar isomer shift (s) and quadrupole splitting parameters (ΔE_Q): s = 1.01(1) mm/s and ΔE_Q = 2.83(2) mm/s for the larger doublet (65(5)%) and s = 0.98(2)(1) mm/s and ΔE_Q = 2.02(6) mm/s for the smaller doublet (35(5)%). The observation of the minor component with similar spectral parameters suggests the presence of Fe(II) sites with slightly different local coordination. This finding is in line with the hypothesis about the partially occupied Na site, since the presence of the Na^+ ions in some positions will produce a slight change in the coordination environment of the Fe(II) centers. In addition, it allows us to evaluate the Na content (x). Each occupied Na site affects two nearby Fe(II) sites (Fig. 3), and the probability to find two Na ions next to any Fe(II) site is very low due to the low SOF of the Na site. Therefore, the 35% contribution of the smaller doublet to the full Mössbauer spectrum corresponds to 17.5% of the (½,0,0) sites being occupied by the Na ions, which is in good agreement with the range of SOF values of 10–20% observed during the refinement of the crystal structure of **1** from X-ray diffraction data.

3.4. Electrical conductivity

It is of interest to compare the crystal structure of **1** to the structures of only a few other coordination compounds in which DMF and TCNQ molecules are coordinated to the metal center, in the absence of capping ligands. The complex $[Fe(DMF)_2(TCNQ)]\cdot 2DMF$, reported by the Dunbar group [30], is a 2D structure composed of $Fe(\mu_4\text{-}TCNQ)$ sheets, with DMF molecules coordinated to the axial positions of the Fe sites. No conductivity measurements were reported for this complex, but the presence of $TCNQ^{2-}$ units suggests that the material should exhibit insulating behavior [45]. In the mononuclear complex $[Zn(TCNQ)_2(H_2O)_2(DMF)_2]$ [46], the Zn^{2+} ion is surrounded by two N atoms of the $TCNQ^-$ anions and for O atoms of the DMF and H_2O molecules. All $TCNQ^-$ anions are η_1-coordinated and form stacks with interplanar distances alternating at 3.195 and 3.291 Å. Magnetic measurements revealed antiferromagnetic coupling between the $TCNQ^-$ anions, but yet again, conductivity measurements were not reported. The conductivity is expected to be low, due to the presence of only integer-charged $TCNQ^-$ anions. Lastly, a series of lanthanide-TCNQ complexes was reported, one of which, $[Gd_2(TCNQ)_2(DMF)_4(H_2O)_{12}](TCNQ)_4\cdot 2DMF$, contains both DMF and H_2O molecules coordinated to the Gd^{3+} ion [47]. This structure also contains only integer-charged $TCNQ^-$ anions. Therefore, even though some of the TCNQ units are organized in stacks, the conductivity is expected to be low. In all the cases described above, transport properties were not explored. In contrast to these structures, the crystal structure of **1**, which contains fractionally charged $TCNQ^{\delta-}$ anions, warrants investigation of its conducting properties.

The 4-probe conductivity measurements were performed on a single crystal of **1** along the [1 1 0] direction, which coincides with the direction of the TCNQ stacks in the crystal structure. The choice of this direction for measurements was facilitated by its coincidence with the longest side of the plate-like crystals. The room-temperature conductivity value of 0.125 S/cm is on the higher side of the typical range observed for semiconductors [48]. It is comparable to the value reported by Dunbar *et al.* for a structurally similar stack of TCNQ anions co-crystallized with a paramagnetic Mn(II) complex [49]. The semiconducting behavior was confirmed by temperature-dependent measurements, which revealed that the resistance (R) increases as the temperature is lowered. The data were fit to a logarithmic dependence, $\ln(R/R_0) = \exp(-E_a/k_BT)$, where R_0 is the room-temperature resistance and E_a is the activation energy for charge hopping, resulting in E_a = 180 meV (Fig. 5).

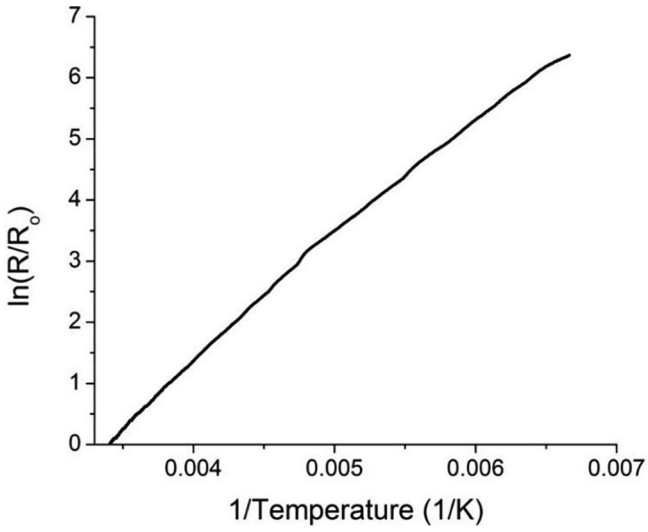

Fig. 5. The dependence of the logarithm of normalized resistance of complex **1** on the inverse temperature, where R_0 represents the resistance at 300 K.

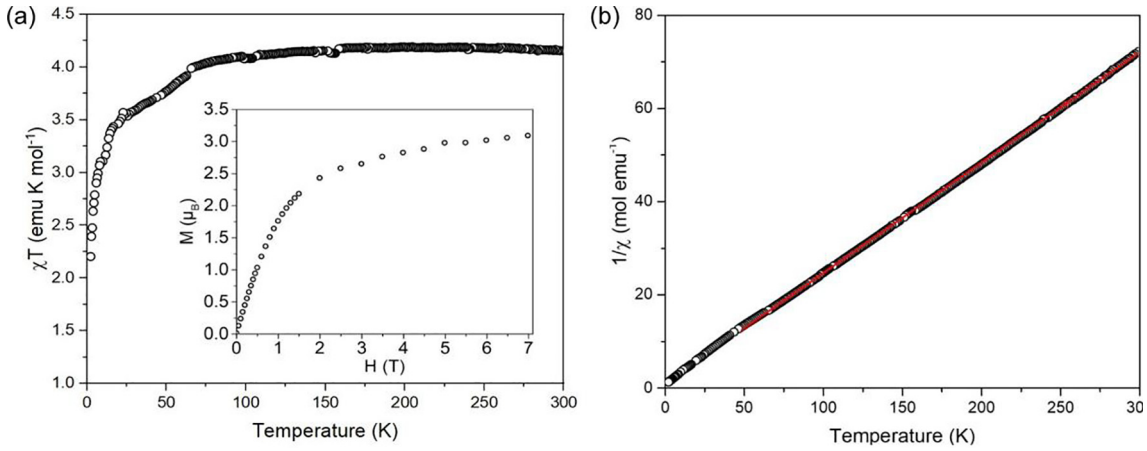

Fig. 6. Magnetic properties of **1**: (a) the temperature-dependent χT product measured at 0.1 T and the field-dependent magnetization at 1.8 K (inset); (b) the Curie-Weiss fit (solid red line) of the inverse magnetic susceptibility. (For interpretation of the references to color in this figure legend, the reader is referred to the web version of this article.)

The plate-like crystals of **1** also showed quite marked deterioration when exposed to air, disintegrating into multiple thinner plates and needles within a few minutes. The effect, most probably, stems from the slow replacement of DMF molecules with H_2O molecules absorbed from moist air. Therefore, the transport measurements had to be performed on a crystal immediately after it has been removed from the mother liquor. If the crystal was exposed to air for a few minutes before attaching the leads, larger resistance values were observed. Likewise, the resistance was observed to gradually increase upon cycling. Interestingly, however, the activation energy remained nearly the same (Fig. S2), suggesting that the increase in the resistance is caused by disintegration of the crystals rather than by the change in the bulk crystal structure.

3.5. Magnetic properties

Magnetic susceptibility measured on a ground polycrystalline sample of **1** revealed a slow decrease in the χT value with temperature (Fig. 6a), from 4.16 emu mol^{-1} K at 300 K to ~ 4.00 emu mol^{-1} K at 70 K. The inverse susceptibility plot (Fig. 6b) was fit to the Curie-Weiss law, $1/\chi = (T - \theta)/C$, giving the Curie constant $C = 4.27(1)$ emu mol^{-1} K and the Weiss constant $\theta = -2.81(2)$ K. The C value is significantly above the range of 3.2–3.8 emu mol^{-1} K, typically observed for the high-spin Fe(II) ion [50], which might be attributed to the additional magnetic contribution from the fractionally charged $TCNQ^{\delta-}$ anions. Below 70 K, the χT quickly decreases, reaching the value of 2.20 emu mol^{-1} K at 1.8 K. This decrease can be attributed to antiferromagnetic coupling between the $TCNQ^{\delta-}$ anions and the Fe(II) centers, as well as to zero-field splitting effects in the latter at lower temperatures. The possibility of antiferromagnetic exchange between the Fe(II) ions and $TCNQ^{\delta-}$ anions is also supported by the field-dependent magnetization measurements at 1.8 K (Fig. 6a, inset). The magnetization does not saturate even at the highest experimentally attainable field of 7 T, reaching the value of 3.1 μ_B, which is significantly lower than 4 μ_B expected for a single high-spin Fe(II) ion. Due to the fractional charge on the $TCNQ^{\delta-}$ anions, it is difficult to assess their total contribution to the magnetization. Availability of a similar model compound with a diamagnetic metal ion is valuable for such an analysis, and efforts are currently under way in our labs to prepare a Zn-containing analog of **1**.

4. Conclusion

This work demonstrates that DMF can be used as effective non-innocent reaction medium for crystallization of charge-transfer complexes of transition-metal ions with fractionally charged $TCNQ^{\delta-}$ anions, in the absence of any additional capping ligands. Due to the fractional charge on the TCNQ units, the title material, $[Fe^{II}(DMF)_4(TCNQ)_2](TCNQ)_2$ (**1**), exhibits high room-temperature conductivity in the direction of the TCNQ stacks observed in its crystal structure. The X-ray crystal structure refinement, the ICP-MS elemental analysis, and Mössbauer spectroscopy provide a strong combined evidence for the presence of a partially occupied Na site in the crystal structure of **1**. Such structural modification is of interest since it modulates the local coordination environment around the Fe(II) centers and, more importantly, the negative charges on the $TCNQ^{\delta-}$ units. The latter effect should influence the low-dimensional conductivity propagated by the columnar stacks of organic anions. Further studies are needed to elucidate such subtle correlations between the crystal structure, electronic properties of the material, and its electrical conductivity. In particular, studies of analogous materials prepared with other transition metal ions and TCNQ precursors, as well as rigorous exclusion or intentional inclusion of Na^+ ions in such preparations, will help shed light on the structure–property relationships in these systems. These investigations are currently under way in our laboratories, and their results will be reported in due course.

Acknowledgments

This research was supported by the National Science Foundation (award CHE-1464955). The Mössbauer and electrical conductivity data were obtained at the National High Magnetic Field Laboratory (NHMFL), which is supported by the NSF Cooperative Agreement (DMR-1157490) and the State of Florida.

Appendix A. Supplementary data

Supplementary data to this article can be found online at https://doi.org/10.1016/j.jmmm.2019.165984.

References

[1] L.B. Coleman, M.J. Cohen, D.J. Sandman, F.G. Yamagishi, A.F. Garito, A.J. Heeger, Solid State Commun. 12 (1973) 1125–1132.
[2] F. Denoyer, F. Comès, A.F. Garito, A.J. Heeger, Phys. Rev. Lett. 35 (1975) 445–449.
[3] J.-P. Farges (Ed.), Organic Conductors: Fundamentals and Applications, CRC Press, New York, 1994.
[4] M.D. Ward, Electroanal. Chem. 16 (1988) 181–312.
[5] M. Bendikov, F. Wudl, D.F. Perepichka, Chem. Rev. 104 (2004) 4891–4945.
[6] U. Geiser, J.A. Schlueter, Chem. Rev. 104 (2004) 5203–5241.
[7] M. Ribault, J.P. Pouget, D. Jérome, K. Bechgaard, J. Phys. Lett. 41 (1980) 607–610.
[8] K. Bechgaard, K. Carneiro, F.B. Rasmussen, M. Olsen, G. Rindorf, C.S. Jacobsen,

H.J. Pedersen, J.C. Scott, J. Am. Chem. Soc. 103 (1981) 2440–2442.
[9] H. Kobayashi, H. Cui, A. Kobayashi, Chem. Rev. 104 (2004) 5265–5288.
[10] Multifunctional Molecular Materials, Pan Stanford Publishing, Singapore, 2013.
[11] E. Coronado, J.R. Galan-Mascaros, J. Mater. Chem. 15 (2005) 66–74.
[12] E. Coronado, P. Day, Chem. Rev. 104 (2004) 5419–5448.
[13] T. Enoki, A. Miyazaki, Chem. Rev. 104 (2004) 5449–5477.
[14] W.E. Broderick, J.A. Thompson, E.P. Day, B.M. Hoffman, Science 249 (1990) 401–403.
[15] W.E. Broderick, D.M. Eichhorn, X. Liu, P.M. Toscano, S.M. Owens, B.M. Hoffman, J. Am. Chem. Soc. 117 (1995) 3641–3642.
[16] R.-M. Lequan, M. Lequan, G. Jaouen, L. Ouahab, P. Batail, J. Padiou, R.G. Sutherland, J. Chem. Soc. Chem. Commun. (1985) 116–118.
[17] L. Ballester, A. Gutiérrez, M.F. Perpiñán, M.T. Azcondo, Coord. Chem. Rev. 190–192 (1999) 447–470.
[18] L. Ballester, A. Gutiérrez, M.F. Perpiñán, S. Rico, M.T. Azcondo, C. Bellitto, Inorg. Chem. 38 (1999) 4430–4434.
[19] L. Ballester, A.M. Gil, A. Gutiérrez, M.F. Perpiñán, M.T. Azcondo, A.E. Sánchez, C. Marzin, G. Tarrago, C. Bellitto, Chem. Eur. J. 8 (2002) 2539–2548.
[20] C. Alonso, L. Ballester, A. Gutiérrez, M.F. Perpiñán, Ana E. Sánchez, M.T. Azcondo, Eur. J. Inorg. Chem. 2005 (2005) 486–495.
[21] L. Ballester, A. Gutiérrez, M.F. Perpiñán, A.E. Sánchez, M. Fonari, M. Gdaniec, Inorg. Chem. 46 (2007) 3946–3955.
[22] R. Clerac, S. O'Kane, J. Cowen, X. Ouyang, R. Heintz, H. Zhao, M.J. Bazile Jr., K.R. Dunbar, Chem. Mater. 15 (2003) 1840–1850.
[23] E.B. Vickers, I.D. Giles, J.S. Miller, Chem. Mater. 17 (2005) 1667–1672.
[24] J.S. Miller, Dalton Trans. (2006) 2742–2749.
[25] A. Nafady, A.P. O'Mullane, A.M. Bond, Coord. Chem. Rev. 268 (2014) 101–142.
[26] H. Zhao, R.A. Heintz, X. Ouyang, K.R. Dunbar, C.F. Campana, R.D. Rogers, Chem. Mater. 11 (1999) 736–746.
[27] B.F. Abrahams, R.W. Elliott, T.A. Hudson, R. Robson, Cryst. Growth Des. 10 (2010) 2860–2862.
[28] B.F. Abrahams, R.W. Elliott, T.A. Hudson, R. Robson, Cryst. Growth Des. 13 (2013) 3018–3027.
[29] B.F. Abrahams, R.W. Elliott, R. Robson, Aus. J. Chem. 67 (2014) 1871–1877.
[30] X. Zhang, M.R. Saber, A.P. Prosvirin, J.H. Reibenspies, L. Sun, M. Ballesteros-Rivas, H. Zhao, K.R. Dunbar, Inorg. Chem. Front. 2 (2015) 904–911.
[31] H. Phan, S.M. Benjamin, E. Steven, J.S. Brooks, M. Shatruk, Angew. Chem. Int. Ed. 54 (2015) 823–827.
[32] J.-Y. Zhang, L.-J. Su, Q.-J. Guo, J. Tao, Inorg. Chem. Commun. 82 (2017) 39–43.
[33] X. Zhang, H. Xie, M. Ballesteros-Rivas, Z.-X. Wang, K.R. Dunbar, J. Mater. Chem. C 3 (2015) 9292–9298.
[34] L.R. Melby, R.J. Harder, W.R. Hertler, W. Mahler, R.E. Benson, W.E. Mochel, J. Am. Chem. Soc. 84 (1962) 3374–3387.
[35] Y. Wang, C. Fang, Y. Huang, Q. Liu, R. Zhao, X. Ding, Y. Huang, RSC Adv. 8 (2018) 24900–24905.
[36] SMART and SAINT, Bruker AXS Inc., Madison, WI, USA, 2007.
[37] G.M. Sheldrick, SADABS, University of Göttingen, Göttingen, Germany, 1996.
[38] G.M. Sheldrick, XPREP. Space group determination and reciprocal space plots, Siemens Analytical X-ray Instruments, Madison, WI, USA, 1991.
[39] G.M. Sheldrick, Acta Crystallogr. Sect. C: Struct. Chem. 71 (2015) 3–8.
[40] C. Prescher, C. McCammon, L. Dubrovinsky, J. Appl. Crystallogr. 45 (2012) 329–331.
[41] G.A. Bain, J.F. Berry, J. Chem. Educ. 85 (2008) 532–536.
[42] V. Coropceanu, J. Cornil, D.A. Da Silva Filho, Y. Olivier, R. Silbey, J.-L. Brédas, Chem. Rev. 107 (2007) 926–952.
[43] H.J. Keller (Ed.), Chemistry and Physics of One-Dimensional Metals, Plenum, 1977.
[44] T.J. Kistenmacher, T.J. Emge, A.N. Bloch, D.O. Cowan, Acta Crystallogr. Sect. B, B 38 (1982) 1193–1199.
[45] B.F. Abrahams, R.W. Elliott, T.A. Hudson, R. Robson, A.L. Sutton, CrystEngComm 20 (2018) 3131–3152.
[46] Y.-C. Chen, H.-B. Zhou, G.-X. Liu, X.-M. Ren, Y. Song, Polyhedron 28 (2009) 1888–1892.
[47] C. Hong, P. Yan, Q. Li, G. Hou, G. Li, J. Organomet. Chem. 739 (2013) 45–51.
[48] C. Kittel, Introduction to Solid State Physics, 8th ed., Wiley, 2005.
[49] M. Ballesteros-Rivas, A. Ota, E. Reinheimer, A. Prosvirin, J. Valdés-Martinez, K.R. Dunbar, Angew. Chem. Int. Ed. 50 (2011) 9703–9707.
[50] M. Shatruk, A. Dragulescu-Andrasi, K.E. Chambers, S.A. Stoian, E.L. Bominaar, C. Achim, K.R. Dunbar, J. Am. Chem. Soc. 129 (2007) 6104–6116.